SCIENCE CHINA
Physics, Mechanics & Astronomy

• Article •

April 2017 Vol. 60 No. 4: 044211
doi: 10.1007/s11433-016-0491-3

Terahertz-dependent evaluation of water content in high-water-cut crude oil using additive-manufactured samplers

LiMei Guan, HongLei Zhan*, XinYang Miao, Jing Zhu, and Kun Zhao*

Beijing Key Laboratory of Optical Detection Technology for Oil and Gas, China University of Petroleum, Beijing 102249, China

Received December 15, 2016; accepted January 10, 2017; published online February 7, 2017

The evaluation of water content in crude oil is of significance to petroleum exploration and transportation. Terahertz (THz) waves are sensitive to fluctuations in the dipole moment of water. However, due to the strong absorption of water in the THz range, it is difficult for the THz spectrum to determine high water content with the common sampler. In this research, micron-grade samplers for THz detection were designed and manufactured using additive manufacturing (AM) technology. Oil-water mixtures with water content from 1.8% to 90.6% were measured with the THz-TDS system using sample cells. In addition, a detailed analysis was performed of the relationships among THz parameters such as signal peak, time delay, and refractive index as well as absorption coefficient and high water content (>60%). Results suggest that the combination of THz spectroscopy and AM technique is effective for water content evaluation in crude oil and can be further applied in the petroleum industry.

water content, crude oil, additive manufacturing, terahertz spectroscopy

PACS number(s): 78.20.Ci, 78.30.Jw, 78.40.Dw

Citation: L. M. Guan, H. L. Zhan, X. Y. Miao, J. Zhu, and K. Zhao, Terahertz-dependent evaluation of water content in high-water-cut crude oil using additive-manufactured samplers, Sci. China-Phys. Mech. Astron. **60**, 044211 (2017), doi: 10.1007/s11433-016-0491-3

1 Introduction

Water content in crude oil is closely related to the prediction of the water level in an oil well, the evaluation of oil reservoir exploitation, and the recovery and development of mining schemes [1]. Therefore, the accurate measurement of water content is significant not only for forecasting the exploiting capacity of an oil field before mining and estimation of working status, but also for grading and evaluating oil products. In addition, the existence of water in crude oil may lead to serious security problems such as pipeline corrosion during the petroleum refining process. There are many methods to detect the water content in crude oil. At present, the most common laboratory methods are centrifugation, distillation, and electrical dewatering [2]. Other approaches such as ray casting, and shortwave, microwave, and capacitance methods, are commonly used for online measurements of water content in crude oil [3,4].

In order to optimize production and confirm integrity, simple and secure methods have been proposed for detecting the water content in crude oil. Terahertz (THz) radiation is a newly developed, non-contact, safe method that can be absorbed by organics and water molecules to varying degrees [5-8]. Because water molecules form labile hydrogen-bond collective networks which are constantly changed on a picosecond time scale [9], the THz spectrum is sensitive to the fluctuations of water dipole moments due to the constant breaking and forming of hydrogen bonds [10]. However, main components of crude oil, such as alkane, have very weak polarity; as a result, THz waves are more weakly absorbed

*Corresponding authors (HongLei Zhan, email: hlzhan@126.com; Kun Zhao, email: zhk@cup.edu.cn)

than water. Accordingly, THz radiation is very sensitive to the change of water content in crude oil. THz spectroscopy technique has been used to detect leaf water content due to the sensitivity of THz to detect slight changes in leaf-tissue water content produced by the closing and opening of stomata [11]. THz spectroscopy is a nondestructive and non-contact method that allows continuous monitoring [9]; thus it is a highly sensitive probe of water content.

Until recently, the use of THz spectroscopy for water content detection has been limited to measurements of samples with relatively low water content, which sometimes can be made into thin slices (as with coal and paper) to reduce the amount of water [12-15]. Our previous report demonstrated a linear relation between absorption coefficient α and water content (0.01%-25%) in emulsions by using samplers with the thickness of 1 mm [16]. We used THz-TDS to characterize 5 oil-water mixtures with water content ranging from 50.05% to 100%; the samples were produced by dropping the mixtures between two pieces of plastic plate. That research was mainly focused on the distribution of oil, gas, and water in high-water-content crude oil mixtures. Measurement accuracy can be improved with smaller measurement intervals and more samples contained by uniform thickness samplers [17].

Precise evaluation of crude oil with water content >60%, known as high-water-cut oil, is affected by the strong absorption of water in the THz range. Significant signal attenuation leads to a decrease in SNR (signal-to-noise ratio), which makes it difficult to detect the THz signal of oil that contains a large amount of water. The effective solution to this problem is to reduce the sample-pool size to micron level.

Rapid prototyping technology is a promising choice for the fabrication of sample cells with high precision and small size. Additive manufacturing (AM), generally known as 3D printing, a rapid prototyping technology of direct digital manufacturing, possesses the advantages of nanometer accuracy and cost efficiency [18-21]. AM is based on the data of a 3D model to rapidly solidify material and fabricate a physical object. AM has been used in the energy industry to print test specimens of rock crevices and joint structures to investigate the stress changes of rocks during mining [22,23]. AM was employed to manufacture models of underground gas channels to guide the development of natural gas fields and to render a print porosity model to characterize pore connectivity before hydraulic exploitation [24]. Because samplers with mm-grade thickness have difficulty measuring samples with water proportions >25% using THz spectroscopy, in the current study we measured the water content in oil-water mixtures ranging from 1.8%-90.6% with specially designed samplers for high-water-content oil that were manufactured with a 3D-printing system. Thus the water content of oil-water mixtures with high water content was quantitatively characterized by the combination of THz spectroscopy and 3D-printing technology.

2 Sample preparation and method

The AM processes start from a software model to fully describe the external geometry (Figure 1). In order to obtain the THz spectra of crude oil with high water content, a 3D-printed cell was used. In our previous work [16], we tested some samples with water content >25% using 1 mm cells, but did not obtain an effective THz signal because of the strong absorption due to the excessive amount of water. Therefore, to improve the SNR, in the current work we designated the thickness of the measured region as 500 μm and the wall as 1000 μm thick. Two holes were placed at the top of the digital cell model for injecting liquid sample and for releasing exhaust gases. The digital models of the cells was designed with pro-engineering and then transported into STL file format (most AM machines accept the STL file format, which has become the standard [25]). The STL file describes the external closed surfaces of the original 3D digital model and forms the basis for calculation of the slices, which can then be successfully read by a 3D printer [26].

Next, the digital model was processed by 3D printer control software into sectional images containing information about the section outline and the filling track. Appropriate printing speed and layer thickness are necessary to the AM system for the following reasons: (1) using higher speed may lead to problems in material solidification and be harmful to the quality of printed product; and (2) applying a thinner layer can reduce physical roughness and reduce system error. Synthetically considering these factors, building parameters such as material constraints, printing speed, and layer thickness were properly set up prior to the printing process; these were Acronitrile-butadiene-styrene (ABS), low speed, and 0.01 cm, respectively. The sample-pool material was heated, melted, and then extruded from the 3D printer's two nozzles for direct printing. The printer we used (XYZ printing da Vinci 2.0, resolution of 100 μm) uses fused deposition modeling technology (FDM), a technique for curing polymer during the 3D printing process. ABS wire rod, a kind of thermoplastic material commonly employed in FDM, was used as the raw material for the sample cells. All of the 27 samples we employed were 3D-printed using the same design model, the same 3D-printing device, and the same printing parameters, in order to shorten the product development cycle and reduce production costs. Analysis of the test area thickness showed that the average relative error was less than 5% and the *Ra* of the surface of the sample cells was 0.1 mm.

For the present research, crude oil with a water content of 1.8% was obtained from Changqing oilfield, China. The oil-water samples were prepared by blending the crude oil with additional water. Water concentrations of various percent-

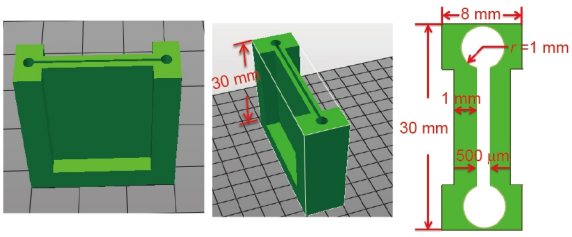

Figure 1 (Color online) 3D model of the sample cell.

ages were calculated *w*/*w* (ratio of water mass to mixture mass). To confirm the uniform distribution of oil and water, the mixtures were stirred for 5 m, immediately injected into the sample cells through the two circular holes, and tested using THz-TDS system. The time period from completed sample to test completion was <1 m.

The THz-TDS system contains a diode-pump mode-locked laser with a repetition of 80 MHz; it generates femtosecond laser pulses whose duration is 100 fs and center wavelength equals 800 nm. The average power of the input laser is <150 mW. The laser pulse is initially split into two beams by the polarization beam splitter to obtain the pump pulse and probe beam. The pump beam is used to generate THz radiation using photoconductive antennas. After being focalized by a lens, the collimated THz pulse transmits into the detection system. The resolution of this system is less than 6 GHz, as reported in one of our previous articles [27]. The THz time-domain spectroscopy (THz-TDS) of each mixture was obtained by this THz transmission system.

In fact, systematic error derived from the instrument and random errors originating in the testing process are unavoidable in the process of an experiment such as this. To minimize the systematic errors in this measurement process, we collected a reference spectrum prior to each sample filling of the cell. The oil-water mixtures were investigated using the corresponding numbered cells and every sample was tested twice at different locations. Moreover, the experiment was conducted under a condition of (21±0.2)°C in dry nitrogen, with humidity <2% to avoid interference by vapor in the air.

3 Results and discussion

Oil-water samples were measured with a THz system. The THz-TDS of the mixtures with varying water cuts show obvious differences (results for selected mixtures are shown in Figure 2, and selected signals with high-water-content samples are shown in the insert). The effective THz waveform of THz signal appears between 18.5 and 25.5 ps. The signal amplitude (E_P) of sample with 1.8% water content reached 88.23 mV, whereas the E_P of crude oil with 90.6% water content is only 23.50 mV. As a whole, the E_P dwindles with the increasing of water content, mainly because water molecules

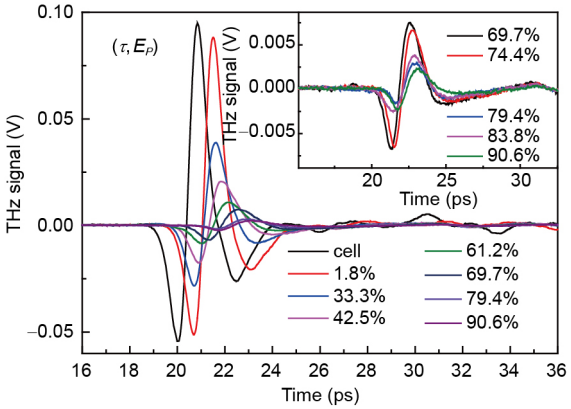

Figure 2 (Color online) THz-TDS of oil-water mixtures with different water contents.

absorb significantly more than crude oil in the THz range. Meanwhile, a phase shift occurs with the augmentation of water content.

The THz-FDS of different water contents were calculated from THz-TDS by FFT (fast Fourier transform algorithm) on the basis of

$$\omega = 2\pi f. \tag{1}$$

The ratio of the sample signal to the empty sample cell signal can be written as:

$$\frac{A_S(\omega)}{A_C(\omega)} = \rho(\omega)\mathrm{e}^{-\mathrm{j}\varphi(\omega)}, \tag{2}$$

where f represents frequency; $\rho(\omega)$ is the module of the ratio; and $\varphi(\omega)$ is the phase of the ratio, which can be calculated by THz-FDS. The refractive index n and absorption coefficient α can be calculated by the following formula:

$$n_S(\omega) = \varphi(\omega)\frac{c_0}{\omega_d} + 1, \tag{3}$$

$$\alpha_S(\omega) = \frac{d}{2}\ln\left[\frac{4n_S(\omega)}{\rho(\omega)(n_S(\omega)+1)^2}\right], \tag{4}$$

where c_0 is the velocity of light in vacuum and d represents the optical path of the sample cell [28]. The frequency-dependent refractive index and absorption coefficient of the oil-water mixtures are shown schematically in Figures 3(a) and (b), respectively. Due to the strong absorption of oil-water mixture, we reduced the effective frequency range to 0.65 THz. We observed that α changed little with the frequency and there is no obvious absorption peak, which is in agreement with the previous report [29]. Here, it is shown that samples with higher water content have greater refractive indices and absorption coefficients.

According to the results above, we can see that there is a relationship between the THz parameter and the water content. To accurately analyze the relationship between them, we separately analyzed the E_P and time delay (τ, the respective transverse coordinate of E_P). Figure 4(a) shows the scatter

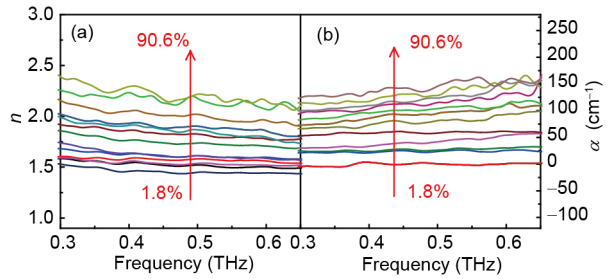

Figure 3 (Color online) (a) Refractive index (n) of different oil-water mixtures; (b) absorption coefficient (α) of different oil-water mixtures.

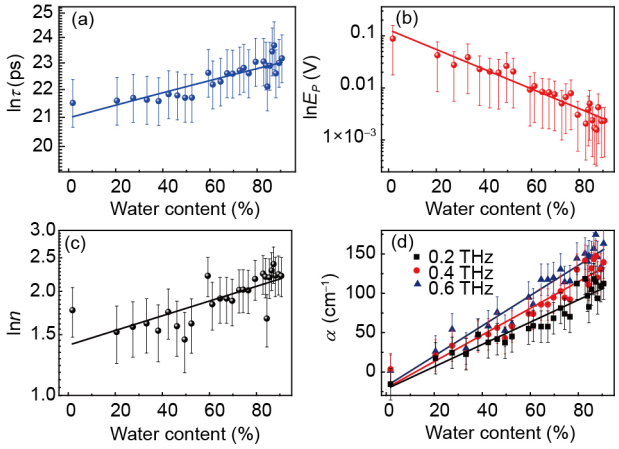

Figure 4 (Color online) (a) lnτ of the oil-water mixtures with water content ranging from 1.8% to 90.6%; (b) lnE_P of the oil-water mixtures with water content ranging from 1.8% to 90.6%; (c) ln$n$ of different water-content oil-water mixtures; (d) α of different water-content oil-water mixtures at 0.2, 0.4, and 0.6 THz.

distribution of τ as well as the water content and Figure 4(b) shows the relationship between E_P and water content. According to the tendency shown in these collected samples, an exponential relationship can be built between τ and water content as well as E_P and water content. E_P decreases with the increase of water content; τ increases with the addition of water. To ensure that the calculations in these error bars did come from multiple measurements, the signal peak and time delay shown in the figures were the average of the two measurements.

We further analyzed the changes of refractive index and absorption as water content according to the refractive index and absorption coefficient of the oil-water mixtures. The results, in Figure 4(c), exhibit exponential damping as the water content in the emulsion increases. We also extracted the absorbance data at selected frequencies. Figure 4(d) shows the water-content-dependent absorption coefficient α of oil-water mixtures at 0.2-0.6 THz with the interval of 0.2 THz. Positive correlation relationships can be built in terms of the absorbance at the selected frequencies. The slopes increase with the augmenting of frequency.

In actual production, the water cut of crude oil in most oilfields, especially in China, has exceeded 60%. For example, the Daqing oilfield has entered the late stage of high-water-cut and the water content is more than 80% [30]. The water cut of crude oil in the Changqing oilfield has already gone over 60%, as it has in the Shengli and Liaohe oilfields [31]. We investigated the relationship of THz response and water content in crude oil with >60% water concentration to simulate the actual conditions in present-day oilfields. A total of 18 samples with water content >60% were analyzed. As shown in Figure 5(a), the E_P of the 3D-printed cells (E_P-cell) were extracted and equal ~96 mV. The relative error is <5% calculated by the equation e=(E_{MAX}–E_{AVE})/E_{AVE}, where E_{MAX} and E_{AVE} represent the maximum value and the average of E_P, respectively, whose errors fall in an acceptable range. In order to improve the accuracy of the analysis and reduce system error, a special THz parameter, the ratio of signal peak, was used as the characterization parameter (Figure 5(b)). Water content was the abscissa; the ordinate was the ratio of E_P of the empty sample cells (E_P-cell) and the oil-water mixtures (E_P-sam). The stars with error bars represent the average E_P ratio of the two measurements. Results show that the E_P ratio decreased with the increasing of water content.

In the process of exploitation and management of oilfields, water content in high-water-cut crude oil is an important technical indicator. THz technique is an effective way to estimate the water content. THz technology can be used to detect high water content due to the vastly different transmission properties of water and crude oil in the THz range. In fact, THz-TDS has been evaluated for discriminating among water contamination levels (0%, 0.1%, and 0.2%) in diesel engine oil. In addition, pure water has been studied using different techniques to observe its properties at THz frequencies. The refractive index values equaled >2 and absorption coefficients were found to be >150 cm^{-1} at 1 THz [32,33]. In addition, THz ATR spectroscopy was used to monitor highly absorbent

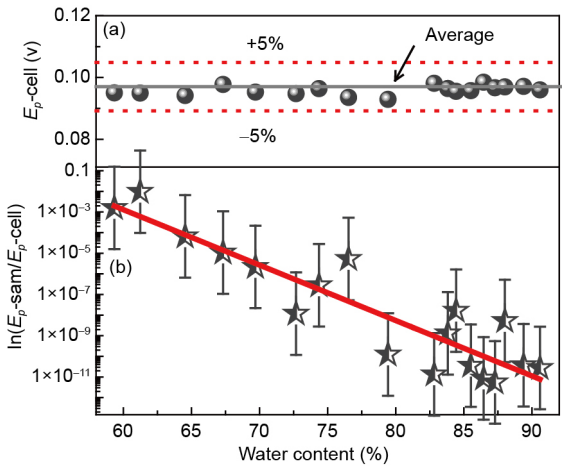

Figure 5 (Color online) Analysis of the mixtures with high water content. (a) E_P of the signal of 3D-printed sample cells; (b) the ratio that takes into account E_P of the empty sample cells (E_p-cell) and the mixtures (E_p-sam).

liquids with water content <40% [34].

The precise measurement of high-water-cut oil, however, is affected by the strong absorption of water in the THz range. In order to solve this problem, all of the standard sample pools in this work were designed and customized with 3D printing technology. The results indicate our initial estimation that the combination of THz spectroscopy and AM technique can be applied in oil characterization, even when the oilfield enters the high-water-bearing period. The added value of our research is the combination of terahertz spectroscopy and AM technology, which has not previously been reported. This combination could be a promising selection for measuring water content of fluid with good accuracy, which in turn could open up a new area of research.

4 Conclusions

We investigated the water content in crude oil by using THz spectroscopy combined with an AM technique, and were able to produce an improved sample cell manufactured by 3D printing that resolved the problem of water content in high-water-cut samples of a common thickness for centimeter-level samplers, which have been generally hard to distinguish in the THz region. Results suggest that THz parameters, including E_P, τ, n, and α, can be used to evaluate water content and that this method is accurate for quantitative analysis of water content in crude oil, even high-water-cut samples. This research represents a new attempt to apply AM technology in the oil exploration and development field. The combination of THz spectroscopy and AM technology seems to be a promising choice for the determination of water content, and the combination of the two technologies will promote innovative applications in oil and gas engineering.

This work was supported by the National Basic Research Program of China (Grant No. 2014CB744302), the Specially Funded Program on National Key Scientific Instruments and Equipment Development (Grant No. 2012YQ140005), the China Petroleum and Chemical Industry Association Science and Technology Guidance Program (Grant No. 2016-01-07), and the National Nature Science Foundation of China (Grant No. 11574401).

1 Z. Zhao, and Y. Wang, Adv. J. Food Sci. Tech. **5**, 76 (2013).
2 M. Fingas, and B. Fieldhouse, Mar. Pollut. Bull. **64**, 272 (2012).
3 O. Lund Bo, and E. Nyfors, J. Non-Cryst. Solids **305**, 345 (2002).
4 M. Zubair, and T. B. Tang, Sensors **14**, 11351 (2014).
5 D. M. Mittleman, Nat. Photon. **7**, 666 (2013).
6 H. L. Zhan, K. Zhao, and L. Z. Xiao, Sci. China-Phys. Mech. Astron. **59**, 644201 (2016).
7 A. D. Burnett, W. Fan, P. C. Upadhya, J. E. Cunningham, M. D. Hargreaves, T. Munshi, H. G. M. Edwards, E. H. Linfield, and A. G. Davies, Analyst **134**, 1658 (2009).
8 C. J. Fecko, J. D. Eaves, J. J. Loparo, A. Tokmakoff, and P. L. Geissler, Science **301**, 1698 (2003).
9 B. L. Yu, Y. Yang, F. Zeng, X. Xin, and R. R. Alfano, Appl. Phys. Lett. **86**, 061912 (2005).
10 D. M. Leitner, M. Gruebele, and M. Havenith, HFSP J. **2**, 314 (2008).
11 E. Castro-Camus, M. Palomar, and A. A. Covarrubias, Sci. Rep. **3**, 2910 (2013).
12 Y. L. Hor, J. F. Federici, and R. L. Wample, Appl. Opt. **47**, 72 (2008).
13 R. Gente, N. Born, N. Voß, W. Sannemann, J. Léon, M. Koch, and E. Castro-Camus, J. Infrared Milli Terahz Waves **34**, 316 (2013).
14 V. Vassilev, B. Stoew, J. Blomgren, and G. Andersson, IEEE Trans. THz Sci. Tech. **5**, 770 (2015).
15 D. Banerjee, W. von Spiegel, M. D. Thomson, S. Schabel, and H. G. Roskos, Opt. Express **16**, 9060 (2008).
16 W. J. Jin, K. Zhao, C. Yang, C. H. Xu, H. Ni, and S. H. Chen, Appl. Geophys. **10**, 506 (2013).
17 Y. Song, H. L. Zhan, K. Zhao, X. Y. Miao, Z. Q. Lu, R. M. Bao, J. Zhu, and L. Z. Xiao, Energy Fuels **30**, 3929 (2016).
18 D. Pires, J. L. Hedrick, A. De Silva, J. Frommer, B. Gotsmann, H. Wolf, M. Despont, U. Duerig, and A. W. Knoll, Science **328**, 732 (2010).
19 M. S. Onses, C. Song, L. Williamson, E. Sutanto, P. M. Ferreira, A. G. Alleyne, P. F. Nealey, H. Ahn, and J. A. Rogers, Nat. Nanotech. **8**, 667 (2013).
20 K. Sun, T. S. Wei, B. Y. Ahn, J. Y. Seo, S. J. Dillon, and J. A. Lewis, Adv. Mater. **25**, 4539 (2013).
21 A. C. Fischer, L. M. Belova, Y. G. M. Rikers, B. G. Malm, H. H. Radamson, M. Kolahdouz, K. B. Gylfason, G. Stemme, and F. Niklaus, Adv. Funct. Mater. **22**, 4004 (2012).
22 Y. Ju, H. Xie, Z. Zheng, J. Lu, L. Mao, F. Gao, and R. Peng, Chin. Sci. Bull. **59**, 5354 (2014).
23 Q. Jiang, X. Feng, Y. Gong, L. Song, S. Ran, and J. Cui, Comp. Geotech. **73**, 210 (2016).
24 S. Ishutov, F. J. Hasiuk, C. Harding, and J. N. Gray, Interpretation **3**, SX49 (2015).
25 A. C. Brown, D. D. Beer, and P. Conradie, S. Afr. J. Ind. Eng. **25**, 39 (2014).
26 M. Wu, J. Tinschert, M. Augthun, I. Wagner, J. Schädlich-Stubenrauch, P. R. Sahm, and H. Spiekermann, Dental Mater. **17**, 102 (2001).
27 H. Zhan, S. Wu, R. Bao, L. Ge, and K. Zhao, Fuel **143**, 189 (2015).
28 W. X. Leng, L. N. Ge, S. S. Xu, H. L. Zhan, and K. Zhao, Chin. Phys. B **23**, 107804 (2014).
29 T. Q. Luong, P. K. Verma, R. K. Mitra, and M. Havenith, Biophys. J. **101**, 925 (2011).
30 D. Gao, J. Ye, Y. Liu, S. Pan, Y. Hu, and H. Yuan, J. Pet. Explor Prod. Tech. **6**, 719 (2016).
31 Y. Shangguan, Y. Zhang, and W. Xiong, Petroleum, **1**, 300 (2015).
32 A. M. Abdul-Munaim, M. Reuter, O. M. Abdulmunem, J. C. Balzer, M. Koch, and D. G. Watson, Trans ASABE **59**, 795 (2016).
33 T. Wang, P. Klarskov, and P. U. Jepsen, IEEE Trans. THz Sci. Tech. **4**, 425 (2014).
34 A. Soltani, S. F. Busch, P. Plew, J. C. Balzer, and M. Koch, J. Infrared Milli Terahz Waves **37**, 1001 (2016).